

Rearrangement of Electron-Rich *N*-Allyldibenzotetraazafulvalenes – An Experimental and Theoretical Study

Christian Holtgrewe,^[a] Christian Diedrich,^[b] Tania Pape,^[a] Stefan Grimme,^{*,[b]} and F. Ekkehardt Hahn^{*,[a]}

Keywords: Benzimidazolin-2-ylidenes / Dibenzotetraazafulvalenes / Allyl substituents / Rearrangement / DFT calculations

The deprotonation of *N*-allylbenzimidazolium halides **9a–d** initially results in the formation of the *N*-allyldibenzotetraazafulvalenes **10**. These electron-rich olefins rearrange to give 1,1',2',3'-tetraalkyl-1',2'-dihydro-2,2'-bibenzimidazoles **13**, either by a 3-aza-Cope rearrangement or by a homolytic *N*-alkyl bond cleavage and addition of the radical at the 2'-position of the bibenzimidazole. Alternatively, double *N*-alkyl bond cleavage gives rise to 1,1'-dialkyl-2,2'-bibenz-

imidazoles **14**. All reaction pathways were studied by use of quantum chemical calculations at the DFT/B3-LYP/TZVP//DFT/BP86/SV(P) level, by comparison of the activation parameters for the radical and the concerted rearrangement mechanisms with the experimentally obtained products.

(© Wiley-VCH Verlag GmbH & Co. KGaA, 69451 Weinheim, Germany, 2006)

Introduction

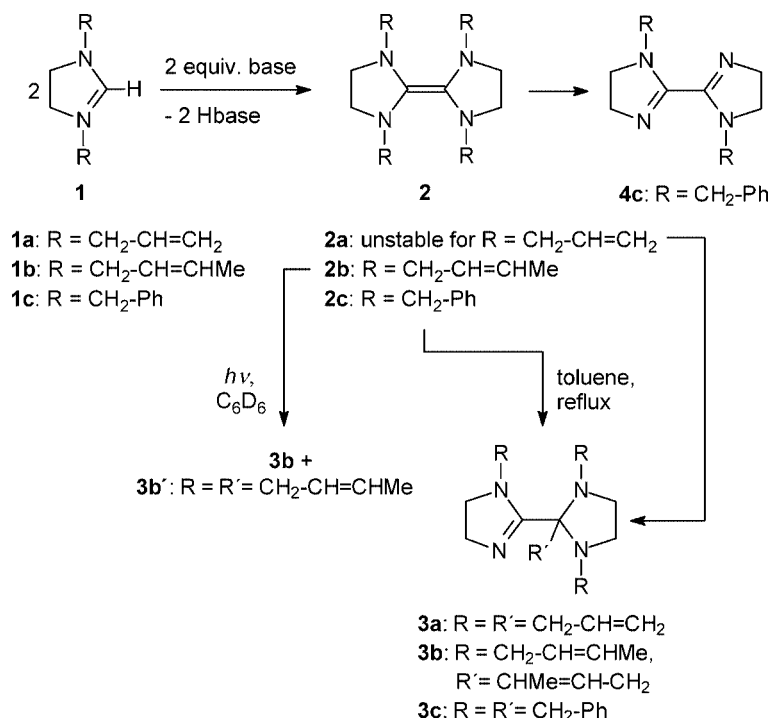
Electron-rich enetetramines have been recognized as powerful reducing agents,^[1] catalysts for the benzoin condensation,^[2] and a source for transition metal carbene complexes.^[3] The cleavage of 2,2'-biimidazolidinylidenes by transition metal complexes had been used for the preparation of various carbene complexes^[4] long before the isolation of the first stable carbenes of the imidazolidin-2-ylidene type by Arduengo et al.^[5] and others.^[6] Alternatively, complexes with imidazolidin-2-ylidene ligands are accessible by treatment of imidazolidinium salts with transition metal complexes containing basic ligands,^[7] by in situ deprotonation of the imidazolidinium salt with an external base, followed by coordination of the formed carbene to a metal center,^[8] or by treatment of the free imidazolidin-2-ylidenes with transition metal complexes.^[9] The last of these methods has been used to substitute phosphane ligands for carbene ligands in a number of transition metal complexes, thereby enhancing their catalytic activity significantly.^[10] The most prominent example of this reaction is the preparation of the type II Grubbs olefin metathesis catalyst, obtained by substitution of a phosphane ligand in [RuCl₂(PR₃)₂(CH–C₆H₅)] for a carbene ligand.^[11]

Complexes with *N*-allyl-functionalized imidazolidin-2-ylidenes have been prepared either by the cyclization of β -functionalized ethyl isocyanides and subsequent alkylation of the ring nitrogen atoms^[12] or by deamination of an *N*¹,*N*³-diallyl-substituted imidazoline amination in the presence of [MCl₂(PR₃)₂] (M = Ni, Pd).^[13] The free *N*¹,*N*³-diallyl-substituted imidazolidin-2-ylidenes or their enetetramine dimers, however, have never been isolated, since the deprotonation of *N,N'*-diallyl-substituted imidazolidinium salts invariably results in the formation of the rearrangement product **3a** (Scheme 1). This rearrangement has been studied in detail for a number of different biimidazolidinylidenes. The 2,2'-biimidazolidinylidene bearing exclusively allyl groups at the ring nitrogen atoms (**2a**: R = CH₂–CH=CH₂) proved to be unstable and spontaneously rearranged to give **3a**.^[14] This rearrangement was believed to be a [3,3]-sigmatropic thermal amino-Claisen reaction, because the rearrangement reaction of the tetracrotlyl derivative (**2b**: R = CH₂–CH=CHMe) regioselectively gave **3b** (R = CH₂–CH=CHMe, R' = CHMe–CH=CH₂). The photochemically induced rearrangement of **2b**, however, gave a mixture of isomers **3b** and **3b'** (**3b'**: R = R' = CH₂CH=CHCH₃). Even the tetrabenzyl-substituted olefin (**2c**: R = CH₂–C₆H₅) rearranged to give **3c** upon heating, most probably by a [1,3]-radical mechanism, as established for the rearrangement of the similar dibenzo-*N,N'*-dibenzylidiazadithiofulvalenes.^[15] Subsequent studies revealed that, in addition to the rearrangement product **3c**, **2c** also yields the dealkylated product **4c** upon heating.^[16]

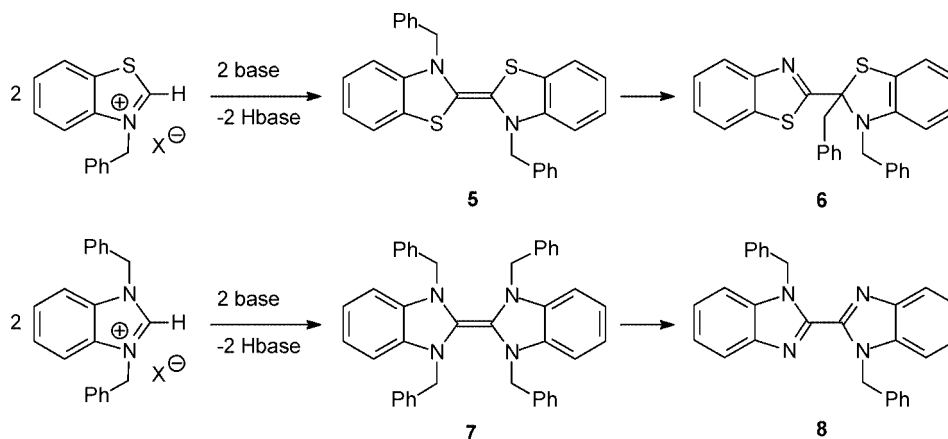
The rearrangement reactivity of benzannulated derivatives of **2** is simpler. *N,N'*-dibenzylidibenzodiazadithiofulvalene **5** rearranges upon heating to give **6**,^[15] which is a derivative of type **3**,^[17] while tetrabenzylidibenzotetraazafulva-

[a] Institut für Anorganische und Analytische Chemie, Westfälische Wilhelms-Universität, Münster, Corrensstraße 36, 48149 Münster, Germany
Fax: +49-251-8333108
E-mail: fehahn@uni-muenster.de

[b] Organisch-Chemisches Institut, Westfälische Wilhelms-Universität Münster, Corrensstraße 40, 48149 Münster, Germany
Fax: +49-251-8336515
E-mail: grimmes@uni-muenster.de



Scheme 1. Rearrangement reactions of electron-rich enetetramines.



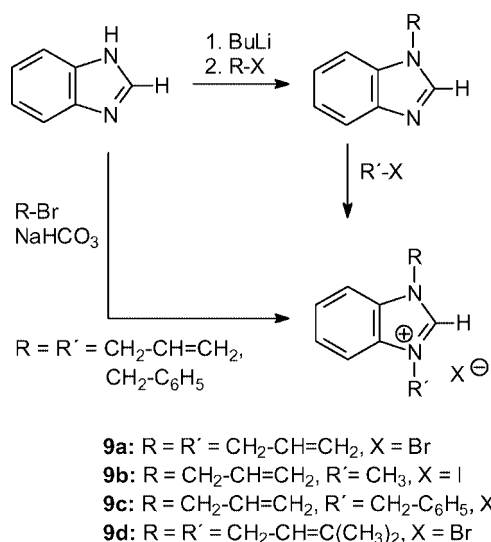
Scheme 2. Rearrangements of dibenzofulvalenes.

lene **7** exclusively yields the debenzilation product **8** (Scheme 2).^[16] The rearrangement reaction of tetraallyldibenzotetraazafulvalene has not been investigated yet.

Although some quantum chemical calculations on the thermodynamics of 3-aza-Cope rearrangements have been reported, tetraazafulvalene systems have yet not attracted much attention;^[18] only one theoretical study dealing with the rearrangement products obtained in the degradation of derivatives of type **2** has been reported.^[14] Here we report DFT calculations and experimental results concerning the synthesis and radical degradation of different *N*-allyl-substituted dibenzotetraazafulvalenes, showing that the [1,3]-radical decomposition pathway is favored for such dimers of benzanulated N-heterocyclic carbenes.

Results and Discussion

The symmetrically *N,N'*-substituted benzimidazolium salts **9a**^[19a] and **9d** (Scheme 3) were prepared in high yields in a one-step procedure, by heating benzimidazole and two equivalents of the appropriate alkyl bromide in acetonitrile in the presence of NaHCO₃. Unsymmetrically *N,N'*-substituted derivatives (**9b**, **9c**)^[19b] were obtained by deprotonation of benzimidazole with *n*BuLi and monoalkylation with allyl bromide. The second alkylation was achieved by treatment of the *N*-allylbenzimidazole with one equivalent of the appropriate alkyl halide. The spectroscopic parameters of **9a–9c** compared well to literature data (Scheme 3).^[19]

Scheme 3. Preparation of the benzimidazolium halides **9a–d**.

The formation of the benzimidazolium bromide **9d** was indicated by the characteristic ^1H NMR resonance of the NCHN proton at $\delta = 10.11$ ppm. The other ^1H NMR and ^{13}C NMR spectroscopic data for **9d** fall in the expected ranges, indicating the desired connectivity. In addition, the molecular features of *N,N'*-diallylbenzimidazolium bromide (**9a**) were established by a single-crystal X-ray diffraction study of crystals grown by slow cooling down of a hot ethanol solution of **9a** to 4 °C. The molecular structure of the cation of **9a** is depicted in Figure 1. The bond lengths in the bicyclic ring system and the angles around the nitrogen atoms indicate aromaticity of the planar rings, whilst the exocyclic double bonds exhibit bond lengths typical of isolated double bonds without conjugation to the ring system.

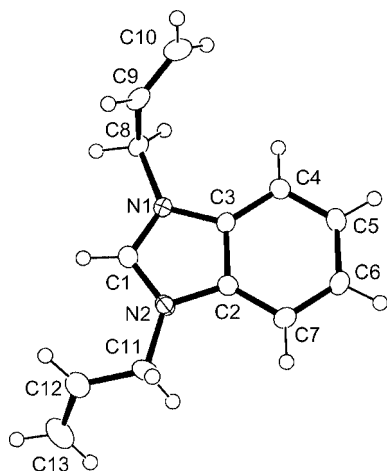


Figure 1. ORTEP drawing of the cation in **9a**. Selected bond lengths [Å] and angles [°]: N1–C1 1.330(2), N1–C3 1.393(2), N2–C1 1.328(2), N2–C2 1.389(2), C9–C10 1.314(3), C12–C13 1.294(3); N1–C1–N2 110.4(2).

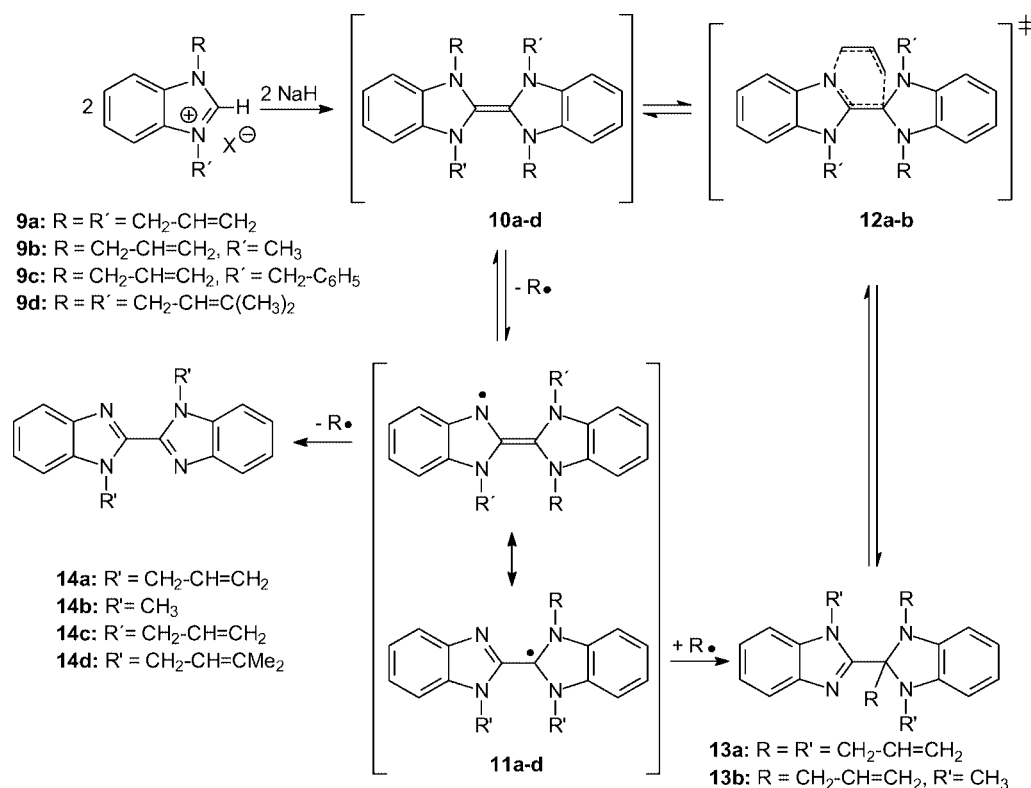
The C2-deprotonation of benzimidazolium salts (or the reductive desulfurization of *N,N'*-alkylated benzimidazole-2-thiones) yields benzimidazolin-2-ylidenes, which can exist as free carbenes when bearing sterically demanding *N*-sub-

stituents^[20a] or as dibenzotetraazafulvalenes with sterically less demanding *N*-substituents.^[20b] The dibenzotetraazafulvalenes are readily cleaved by coordinatively unsaturated transition metal complexes, to give carbene complexes.^[20b,21] Benzimidazolium salts^[22] – including *N*-allyl-substituted ones^[22b,c] – react with transition metal complexes containing basic ligands with C2-deprotonation and formation of carbene complexes. No dibenzotetraazafulvalenes, however, could be isolated upon deprotonation of the benzimidazolium salts **9a–d**, in which C2-deprotonation initially yields the dibenzotetraazafulvalenes **10a–d**, which are not stable but instead either rearrange (to compounds of type **13**) or decompose (to compounds of type **14**) with cleavage of one or two exocyclic *N*–*R* bonds, depending on the type of *N*-substituents (Scheme 4).

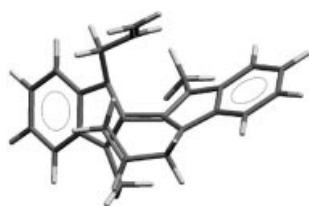
The rearrangement products **13a–b** can be formed from the dibenzotetraazafulvalenes **10a–b** in two different ways. The radical pathway involves the loss of one allyl radical with formation of the benzimidazolyl radicals **11a–b**, which can then recombine with the allyl radical in the C2' position to give the rearrangement products **13a–13b**. Alternatively, particularly in cases of α,β' -unsaturated systems such as **10a–b**, a 3-aza-Cope rearrangement is possible, also giving **13a–b** via the six-membered transition state **12a–b**. Rearrangement products of type **13** were not obtained when starting from **9c** and **9d** (vide infra).

In order to establish the reaction mechanism for the formation of the rearrangement products **13a–13b**, the transition state energies of the sigmatropic rearrangement (**12a–b**) were compared with the energies of the radical pairs **11a–11b**, which represent the intermediates on the radical pathway. This implies the reasonable assumption that the homolytic bond cleavage resulting in the formation of the radicals of type **11** is “barrier-less”, such that the corresponding dissociation (reaction) energy reflects the activation energy of the overall process.

In the unsubstituted model system $\text{H}_2\text{C=CH-N-CH}_2\text{-CH=CH}_2$, the transition state for the 3-aza-Cope rearrangement adopts an almost “strainless” chairlike structure. Given the very rigid backbones of the dibenzotetraazafulvalenes and the steric demands of the residues *R* and *R'*, one might expect that the activation energies for the sigmatropic rearrangements ($\Delta E^\ddagger_{\text{C}}$) of these derivatives would be substantially higher than that of the chain-like unsubstituted derivative. However, the activation energies obtained at the DFT/B3-LYP/TZVP//DFT/BP86/SV(P) (in the following abbreviated as B3LYP/TZVP) level are remarkably similar for the unsubstituted system and for the dibenzotetraazafulvalenes bearing four (**10a**) or two (**10b**) *N*-allyl substituents (Table 1 and Figure 2). It appears logical that the more bulky allyl/benzyl or 3-methylbut-2-enyl *N,N'*-substituents in **10c** and **10d** should not cause any reduction in the activation energy, but the two corresponding transition states could not be obtained theoretically, which might be due to technical reasons. However, this behavior also indicates that, because of the sterically demanding substituents in **10c–d**, there is no pathway on the potential energy hypersurface that would allow a sigmatropic rearrangement.

Scheme 4. Rearrangement and decomposition of *N*-allyl-substituted dibenzotetraazafulvalenes.Table 1. Calculated activation energies (B3-LYP/TZVP) for the 3-aza-Cope rearrangement (ΔE_C^\ddagger) and for the radical rearrangement (ΔE_R) of **12a-d** in kcal·mol⁻¹.

Entry	ΔE_C^\ddagger	ΔE_R	$\Delta \Delta E$
10a: R = R' = CH ₂ -CH=CH ₂	37.8	10.0	27.8
10b: R = CH ₂ -CH=CH ₂ , R' = CH ₃	38.2	8.7	29.5
10c: R = CH ₂ -CH=CH ₂ , R' = CH ₂ -C ₆ H ₅	not determined	11.1	not determined
10d: R = R' = CH ₂ -CH=C(CH ₃) ₂	not determined	6.8	not determined
H ₂ C=CH-N-CH ₂ -CH=CH ₂	38.8	52.1	-13.3

Figure 2. Calculated structure of the transition state **12b**.

In contrast with the small changes in the activation energy observed for the sigmatropic rearrangements, the energetics of the radical pathway undergo substantial changes depending on the *N*-substitution pattern. For the 3-aza-Cope rearrangement of the hypothetical unsubstituted molecule the formation of the radical pair requires an energy of around 52 kcal·mol⁻¹ and therefore cannot compete with the concerted rearrangement. The radical pairs resulting from the *N*-allyl bond cleavage of the dibenzotetraazafulvalenes **10a** and **10b**, on the other hand, are stabilized by the large aromatic backbone, so the radical pathway is strongly favored (Table 1). For the benzylic-substi-

tuted (**10c**) and the 3-methylbut-2-enyl-substituted (**10d**) systems the same reasons hold, which is confirmed by the very similar energies needed for the formation of the respective radical pairs (Table 1). However, no recombination of the radicals to give compounds of type **13** was observed for these radical pairs (vide infra).

In summary, the radical pathway is favored for the formation of **13a-b** from dibenzotetraazafulvalenes **10a-b** because of the high stabilities of the bibenzimidazolyl radicals of type **11a-b** relative to their unsubstituted counterpart. The activation barriers of the corresponding sigmatropic rearrangements are of the same order of magnitude as for the unsubstituted system.

In addition, the bibenzimidazolyl radicals of type **11** are capable of decomposing through a second deallylation or debenzoylation to yield the 2,2'-connected bibenzimidazoles **14a-d** (Scheme 4). The allylic radicals abstracted from compounds of type **11** react with the solvent (THF) to form propene and a THF radical. Two of these THF radicals recombine afterwards to generate a dimer of THF, which could be identified in the reaction product by GC/MS. The

2,2'-bibenzimidazoles **14a–d** (note that compounds **14a** and **14c** are identical, as the double debenzylation of **10c** proceeds more rapidly than a double deallylation) could be isolated for the first time, together with the rearrangement products (**13a** and **13b**), by column chromatography from one reaction. The decomposition products of type **14** are air-stable, colorless solids, showing intense fluorescence at 254 nm. They were identified by NMR spectroscopy, showing resonances similar to the already known substituted benzimidazoles.^[23]

The molecular structures of the decomposition products **14a** and **14b** have been established by single-crystal X-ray diffraction analysis (Figure 3). The molecular structure of **14b** derived from an incomplete data set has been reported previously.^[24] Both compounds crystallize in centrosymmetric monoclinic space groups with the midpoints of the N₂C–CN₂ bonds residing on crystallographic inversion centers. Both **14a** and **14b** exhibit almost perfectly planar molecular geometries. Bond lengths and bond angles in the tetracyclic

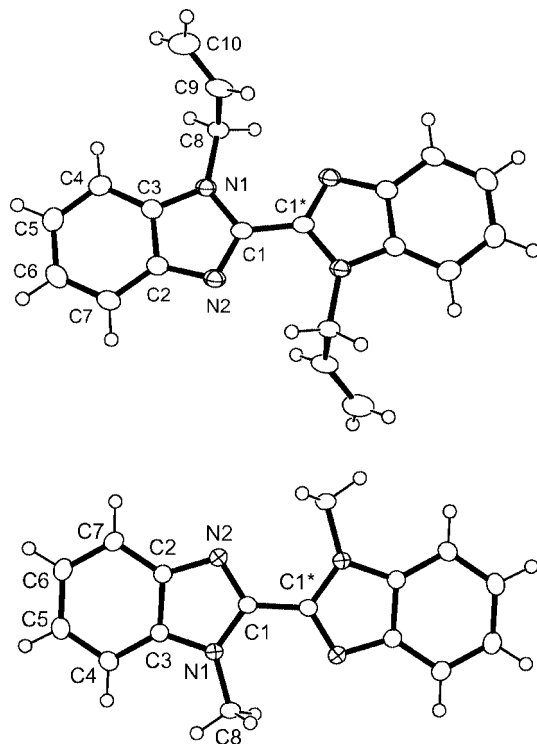


Figure 3. ORTEP drawing of the molecular structures of **14a** (top) and **14b** (bottom). Selected bond lengths [Å] and angles [°] for **14a** [**14b**]: N1–C1 1.378(2) [1.375(1)], N1–C3 1.378(2) [1.376(1)], N2–C1 1.325(2) [1.323(1)], N2–C2 1.381(2) [1.380(1)], C1–C1* 1.459(3) [1.457(2)]; N1–C1–N2 113.03(12) [113.30(8)].

systems of both molecules show that polarized aromatic π -systems are present, each extending over the whole molecule. The C=C bonds of the *N*-allyl groups in **14a** are typical of localized double bonds without electronic interaction with the aromatic ring system.

In order to gain some insight into the processes that eventually result in the decomposition (**10**→**14**) or the rearrangement (**10**→**13**), the reaction energies required for the formation of the different radical intermediates were calculated, together with the overall reaction energies. In the cases of the bibenzimidazolyl radicals **11a** ($R = R' = \text{CH}_2\text{--CH=CH}_2$) and **11b** ($R = \text{CH}_2\text{--CH=CH}_2$, $R' = \text{CH}_3$) the rearrangement products **13a** and **13b** were isolated together with the deallylation products **14a** and **14b**. The reaction energies for the radical decomposition (ΔE_{rD}) and the radical rearrangement (ΔE_{rR}) show that, from a thermodynamic point of view, deallylation (**10**→**14**) is strongly favored over the radical rearrangement (**10**→**13**). The observation that, in spite of this situation, both products are found experimentally can very probably be attributed to the fact that the back-reaction from **13a** and **13b** to the radical pair is rather slow under the reaction conditions, so **13a** and **13b**, once formed, are kinetically trapped, so the product distribution does not reflect the thermodynamic considerations (Table 2).

In the case of the *N*-allyl-*N'*-benzylbibenzotetraazafulvene **10c**, three different decomposition reactions are conceivable: *i*) double deallylation, *ii*) double debenzylation, and *iii*) mixed deallylation-debenzylation. The thermodynamics of these reactions were examined by calculating the reaction energies for the two homodealkylations, and assuming that the third possible reaction – the heterodealkylation – should energetically lie in between the other two. To predict the product distribution between the two above homodealkylations, the activation energies of both processes were estimated by calculating the energies for the abstraction of the first radical ($\Delta E_{\text{AA}}^{\text{a}}$ for the allyl radical abstraction, $\Delta E_{\text{BB}}^{\text{a}}$ for the benzyl radical abstraction). In addition, the reaction energies for the two possible homodealkylations (ΔE_{AA} for the deallylation, ΔE_{BB} for the debenzylation) were determined (Table 3). The data show that no significant differences exist (in the gas phase) either for the first N–C cleavage reaction or in the total reaction energies of these two reactions, so a mixture of the different dealkylation products should have been obtained from the decomposition of **10c**. Experimentally, though, only the debenzylated reaction product **14c** was found, indicating that solvent effects and other influences not taken into account in our theoretical treatment in the gas phase are of some importance.

Table 2. Calculated reaction energies (B3-LYP/TZVP) for the radical degradation (including formation of one THF dimer) and rearrangement of compounds **10a–b** in kcal·mol^{−1}.

Entry	ΔE_{rD} (10 → 14)	ΔE_{rR} (10 → 13)	$\Delta \Delta E_{\text{rRD}}$
10a : $R = R' = \text{CH}_2\text{--CH=CH}_2$	−59.8	−27.9	31.9
10b : $R = \text{CH}_2\text{--CH=CH}_2$, $R' = \text{CH}_3$	−61.6	−27.0	34.6

Table 3. Calculated energies for the first N–C cleavage reaction of **10c** and total reaction energy (including formation of one THF dimer) for the conversion of **10c** (B3-LYP/TZVP) in kcal·mol^{−1}.

Deallylation	$\Delta E_{AA}^a = 10.8$	$\Delta E_{AA} = -61.9$
Debenzylation	$\Delta E_{BB}^a = 11.1$	$\Delta E_{BB} = -63.0$

The decomposition reaction of the *N*-3-methylbut-2-enyl-substituted dibenzotetraazafulvalene [**10d**, R = R' = CH₂–CH=C(CH₃)₂] indicates that kinetic effects play an important role in the radical chemistry of this kind of electron-rich double bond system. The activation energy for the first homolytic bond cleavage, among all the dibenzotetraazafulvalenes of type **10**, was calculated to be smallest for **10d** (ΔE_R **10d**→**11d** = 6.8 kcal·mol^{−1}, Table 1, Scheme 4), indicating that **10d** should react by the radical pathway. Two subsequent reactions are possible after formation of **11d**: recombination of the radicals with formation of a compound of type **13** and cleavage of a second N–C bond to give **14d** (Scheme 5).

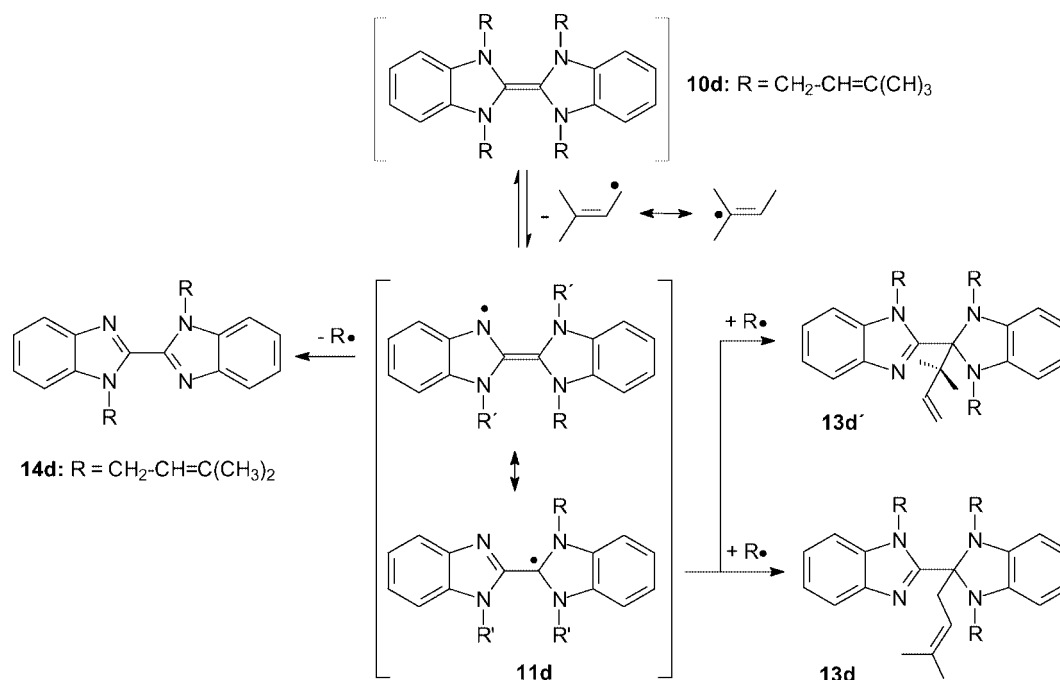
Because of the asymmetric nature of the 3-methylbut-2-enyl radical, the recombination of the radical pair can theoretically yield two different products: **13d** and **13d'** (Scheme 5). Compound **13d** would be the result of recombination with the unsubstituted tail of the 3-methylbut-2-enyl radical, and **13d'** would be formed in recombination through the tertiary carbon atom of the radical. The reaction energies for both possible rearrangements (ΔE_{4MB}) were calculated and were compared with the reaction energy for the second N–C cleavage to give **14d**. The reaction energy for this last process was calculated with respect to

the formation of a THF dimer from the abstracted 3-methylbut-2-enyl radical (Table 4).

Table 4. Calculated reaction energies (B3-LYP/TZVP) for the reactions of **10d** in kcal·mol^{−1}.

Entry	ΔE_{4MB}
10d → 13d'	−7.1
10d → 13d	−26.9
10d → 14d	−60.8

The reaction energies for the three different reactions of the dibenzotetraazafulvalene **10d** show that the rearrangement yielding **13d'** would be unlikely to happen, because it is only slightly exothermic (−7.1 kcal·mol^{−1}). This rearrangement appears to be hindered by steric effects. The reaction energies of the other two reactions are more exothermic and both reactions could occur, as was observed with the other *N*-allyl-substituted dibenzotetraazafulvalenes (**10a–b**, Table 2). While the transformation **10d**→**14d** is more exothermic than the reaction **10d**→**13d**, the difference in the reaction energies ($\Delta\Delta E_{4MB} = 33.9$ kcal·mol^{−1}) is similar to the values observed for alternative reactions of the dibenzotetraazafulvalenes **10a–b** ($\Delta\Delta E_{TRD} = 31.9$ kcal·mol^{−1} for **10a**, $\Delta\Delta E_{TRD} = 34.6$ kcal·mol^{−1} for **10b**, Table 2). From a thermodynamic point of view, both **13d** and **14d** should be accessible from **10d**, but experimentally only the degradation product **14d** was obtained. This behavior can be interpreted by the qualitative arguments given above for the simultaneous formation of **13a/14a** and **13b/14b**. We concluded that the product distribution is to a large extent determined by the reaction rates and so does not reflect what would be expected from thermodynamics.



Scheme 5. Possible reactions of dibenzotetraazafulvalene **11d**.

Conclusions

We have demonstrated that *N*-allyl-substituted dibenzotetraazafulvalenes react through rearrangement and dealkylation reactions. DFT calculations revealed that the rearrangement most probably proceeds by a radical pathway and not through a concerted 3-aza-Cope reaction. Comparison of the theoretical results with the experimentally found product distributions of the dealkylation reactions demonstrated that kinetic effects play an important role in the decomposition of *N*-allyldibenzotetraazafulvalenes.

Experimental Section

General: If not noted otherwise all manipulations were carried out under purified argon in Schlenk flasks. Solvents were dried with Na/benzophenone (THF, diethyl ether, toluene) or CaH₂ (CH₂Cl₂). The benzimidazolium halides **9a–c** were prepared by methods adapted from literature procedures (symmetrical derivative **9a**,^[19a] unsymmetrical derivatives **9b**^[19b] and **9c**^[19b]). Elemental analyses (C, H, N) were performed with a Vario EL Elemental Analyzer at the Institut für Anorganische und Analytische Chemie, Universität Münster.

1,3-Bis(3-methylbut-2-enyl)benzimidazolium Bromide (9d): Benzimidazole (7.0 g, 60 mmol), NaHCO₃ (5.04 g, 60 mmol), and 1-bromo-3-methylbut-2-ene (22.5 g, 150 mmol) were added to acetonitrile (120 mL). The mixture was heated under reflux for 24 h. The solvent was removed in vacuo and the brown residue was suspended in hot ethanol (25 mL). Solids were removed by filtration of the hot suspension. Upon cooling to 4 °C compound **9d** precipitated as colorless needles. 15.8 g (79%). ¹H NMR (200 MHz, CDCl₃): δ = 10.11 (s, 1 H, NCHN), 7.64–7.53 (m, 4 H, Ar–H), 5.41 [t, ³J_{H,H} = 7.01 Hz, 2 H, CH₂CH=C(CH₃)₂], 5.16 [d, ³J_{H,H} = 7.01 Hz, 4 H, CH₂CH=C(CH₃)₂], 1.87 [s, 6 H, CH=C(CH₃)₂], 1.75 [s, 6 H, CH=C(CH₃)₂] ppm. ¹³C NMR (50 MHz, CDCl₃): δ = 141.3 [CH₂CH=C(CH₃)₂], 131.6 (NCHN), 126.8 (Ar-C_{ipso}), 124.7 (Ar-C_{meta}), 115.3 (Ar-C_{ortho}), 113.1 [CH₂CH=C(CH₃)₂], 45.6 [CH₂CH=C(CH₃)₂], 24.8, 20.3 [CH₂CH=C(CH₃)₂] ppm. C₁₇H₂₃N₂Br (335.29): calcd. C 60.90, H 6.91, N 8.36; found C 61.23, H 7.19, N 8.55.

General Procedure for the Deprotonation and Rearrangement of *N*-Allyl-Substituted Benzimidazolium Halides: A benzimidazolium halide **9a–d** (4 mmol) was suspended in THF (20 mL). Sodium hydride (96 mg, 4 mmol) was added and the reaction mixture was stirred for two hours at ambient temperature. Subsequently, the solvent was removed in vacuo and the brownish residue was suspended in toluene (20 mL). Solids were removed by filtration and the filtrate was taken to dryness. The reaction products were isolated as colorless crystals after column chromatography (SiO₂, *n*-hexane/ethyl acetate, 1:1) and recrystallization from (*n*-hexane/ethyl acetate, 1:1).

1,1',2',3'-Tetra(prop-2-enyl)-1',2'-dihydro-2,2'-bibenzimidazole (13a): Yield: 340 mg (43%). ¹H NMR (400 MHz, CDCl₃): δ = 7.87 (m, 2 H, Ar–H), 7.38 (m, 6 H, Ar–H), 6.58 (m, 1 H, CH₂CH=CH₂), 6.32 (m, 1 H, CH₂CH=CH₂), 6.05 (m, 2 H, CH₂CH=CH₂), 5.61 (m, 4 H, NCH₂CH=CH_{trans}), 5.06 (m, 4 H, NCH₂CH=CH_{trans}), 3.58 (m, 6 H, NCH₂CH=CH_{trans}), 2.21 (m, 2 H, CCH₂CH=CH₂) ppm. ¹³C NMR (100 MHz, CDCl₃): δ = 151.8 (NC=N), 142.6, 139.2, 135.4, 133.0 (Ar-C_{ipso}), 133.9, 132.3, 132.2 (CH₂CH=CH₂), 123.8, 122.7 (Ar-C_{meta}), 122.1, 123.3, 119.2, 117.9 (CH₂CH=CH₂), 117.6, 117.2 (Ar-C_{meta}), 117.0, 110.6, 103.0 (Ar-

ortho), 87.7 (NCH₂CN), 47.6, 47.4, 46.4, 30.7 (CH₂CH=CH₂) ppm. MS (EI = 70 eV): *m/z* (%) = 355 (10) [M – C₃H₅]⁺, 314 (50) [M – 2C₃H₅]⁺, 273 (100) [M – 3C₃H₅]⁺. C₂₆H₂₈N₄ (396.54): calcd. C 78.75, H 7.12, N 14.13; found C 78.44, H 7.33, N 14.23.

1,3'-Dimethyl-1',2'-di(prop-2-enyl)-1',2'-dihydro-2,2'-bibenzimidazole (13b): Yield: 186 mg (27%). ¹H NMR (400 MHz, CDCl₃): δ = 7.84 (dd, 1 H, Ar–H), 7.34 (m, 3 H, Ar–H), 6.61 (m, 2 H, Ar–H), 6.31 (dd, 1 H, Ar–H), 6.22 (dd, 1 H, Ar–H), 5.85 (m, 2 H, CH₂CH=CH₂), 5.73 (m, 2 H, CH₂CH=CH₂), 5.24 (dm, ³J_{H,H} = 16.8 Hz, 1 H, NCH₂CH=CH_{trans}), 5.12 (dm, ³J_{H,H} = 17.4 Hz, 1 H, CCH₂CH=CH_{trans}), 5.05 (dm, ³J_{H,H} = 10.0 Hz, 1 H, NCH₂CH=CH_{cis}), 4.98 (dm, ³J_{H,H} = 10.4 Hz, 1 H, CCH₂CH=CH_{cis}), 3.73 (dm, ³J_{H,H} = 6.8 Hz, 2 H, NCH₂CH=CH₂), 3.67 (s, 3 H, CH₃), 3.45 (dm, ³J_{H,H} = 6.6 Hz, 2 H, CCH₂CH=CH₂), 2.97 (s, 3 H, CH₃) ppm. ¹³C NMR (100 MHz, CDCl₃): δ = 152.2 (NC=N), 141.3, 139.9, 139.5, 137.5 (Ar-C_{ipso}), 133.7, 131.9 (CH₂CH=CH₂), 123.2, 122.1 (Ar-C_{meta}), 120.1, 119.2 (CH₂CH=CH₂), 118.1 (Ar-C_{ortho}), 117.6, 117.2 (Ar-C_{meta}), 109.3, 102.5, 101.5 (Ar-C_{ortho}), 87.3 (NCH₂CN), 46.0 (NCH₂CH=CH₂), 39.0 (CCH₂CH=CH₂), 30.8, 27.8 (CH₃) ppm. C₂₂H₂₄N₄ (344.46): calcd. C 76.71, H 7.02, N 16.27; found C 76.61, H 7.38, N 16.01.

1,1'-Di(prop-2-enyl)-2,2'-bibenzimidazole (14a): Yield: 219 mg (35%). ¹H NMR (200 MHz, CDCl₃): δ = 7.87 (m, 2 H, Ar–H), 7.48 (m, 2 H, Ar–H), 7.38 (m, 4 H, Ar–H), 6.03 (m, 2 H, NCH₂CH=CH₂), 5.60 (d, ³J_{H,H} = 9.6 Hz, 2 H, NCH₂CH=CH_{cis}), 4.88 (m, 6 H, NCH₂CH=CH₂ and NCH₂CH=CH_{trans}) ppm. ¹³C NMR (50 MHz, CDCl₃): δ = 142.8, 144.4 (Ar-C_{ipso}), 137.5 (NCN), 133.2 (NCH₂CH=CH₂), 124.1, 123.9 (Ar-C_{meta}), 118.6 (NCH₂CH=CH₂), 110.9, 109.8 (Ar-C_{ortho}), 40.8 (NCH₂CH=CH₂) ppm. MS (EI = 70 eV): *m/z* (%) = 314 (20) [M]⁺, 273 (100) [M – C₃H₅]⁺, 258 (10), 234 (10), 144 (10), 102 (10), 77 (15) [C₆H₅]⁺. C₂₀H₁₈N₄ (314.39): calcd. C 76.41, H 5.77, N 17.82; found C 76.57, H 5.79, N 17.64.

1,1'-Dimethyl-2,2'-bibenzimidazole (14b): Yield: 230 mg (44%). ¹H NMR (200 MHz, CDCl₃): δ = 7.87 (dd, 2 H, Ar–H), 7.39 (m, 6 H, Ar–H), 4.33 (s, 6 H, CH₃) ppm. ¹³C NMR (50 MHz, CDCl₃): δ = 143.2, 143.5 (Ar-C_{ipso}), 136.2 (NCN), 123.9, 122.8 (Ar-C_{meta}), 120.2, 110.0 (Ar-C_{ortho}), 32.4 (CH₃) ppm. C₁₆H₁₄N₄ (262.31): calcd. C 73.26, H 5.38, N 21.36; found C 73.51, H 5.32, N 21.17.

1,1'-Bis(3-methylbut-2-enyl)-2,2'-bibenzimidazole (14d): Yield: 206 mg (28%). ¹H NMR (400 MHz, CDCl₃): δ = 7.78 (dd, 2 H, Ar–H), 7.26 (m, 4 H, Ar–H), 6.96 (dd, 1 H, Ar–H), 6.85 (dd, 1 H, Ar–H), 5.42 [d, ³J_{H,H} = 6.8 Hz, 4 H, NCH₂CH=C(CH₃)₂], 5.19 [t, ³J_{H,H} = 6.8 Hz, 2 H, CH₂CH=C(CH₃)₂], 1.68, 1.63 (s, 6 H, CH₃) ppm. ¹³C NMR (100 MHz, CDCl₃): δ = 142.9, 142.8 (Ar-C_{ipso}), 135.7 (NCN), 123.6, 122.6 (Ar-C_{meta}), 119.9 [NCH₂CH=C(CH₃)₂], 110.6, 107.8 (Ar-C_{ortho}), 43.6 [NCH₂CH=C(CH₃)₂], 24.6 [NCH₂CH=C(CH₃)₂] ppm. MS (EI = 70 eV): *m/z* (%) = 370 (60) [M]⁺, 301 (100). C₂₄H₂₆N₄ (370.50): calcd. C 77.80, H 7.07, N 15.12; found C 78.05, H 7.12, N 14.83.

X-ray Crystallography: Diffraction data for **9a**, **14a**, and **14b** were collected with a Bruker AXS APEX CCD diffractometer fitted with a rotating anode at 123(2) K (for **9a**) and 173(2) K (for **14a** and **14b**) with use of graphite monochromated Mo-K_α radiation. Data were collected over the full sphere and were corrected for absorption. Structure solutions were found by the Patterson method or by Direct Methods. Structure refinement was carried out by full-matrix, least-squares on *F*² with SHELXL-97^[25] by use of first isotropic and later anisotropic displacement parameters for all non-hydrogen atoms. Hydrogen atom positions were observed or calculated and refined riding on carbon atoms.

Compound 9a: C₁₃H₁₅N₂Br, *M* = 279.18, colorless needle 0.15 × 0.10 × 0.06 mm, *a* = 8.2249(5), *b* = 8.5731(5), *c* = 10.0351(6) Å, *α* = 97.4150(10), *β* = 105.6870(10), *γ* = 110.0270(10)°, *V* = 620.54(6) Å³, *ρ*_{calc} = 1.494 g·cm⁻³, *μ* = 3.287 mm⁻¹, *Z* = 2, triclinic space group *P* $\bar{1}$ (no. 2), Mo-*K*_α radiation, *λ* = 0.71073 Å, *T* = 123(2) K, 6104 reflections collected (*±h*, *±k*, *±l*), [(*sin θ*)/*λ*] = 0.65 Å⁻¹, 2827 independent (*R*_{int} = 0.0218) and 2655 observed reflections [*I* ≥ 2 *σ*(*I*)], 145 refined parameters, *R* = 0.0271, *wR*₂ = 0.0654 (all intensities), max. residual electron density 0.725 (−0.416) e·Å⁻³.

Compound 14a: C₂₀H₁₈N₄, *M* = 314.38, colorless needle 0.50 × 0.05 × 0.02 mm, *a* = 4.5678(10), *b* = 19.169(4), *c* = 8.984(2) Å, *β* = 95.631(4)°, *V* = 782.9(3) Å³, *ρ*_{calc} = 1.334 g·cm⁻³, *μ* = 0.082 mm⁻¹, *Z* = 2, monoclinic space group *P*2₁/*c* (no. 14), Mo-*K*_α radiation, *λ* = 0.71073 Å, *T* = 173(2) K, 6000 reflections collected (*±h*, *±k*, *±l*), [(*sin θ*)/*λ*] = 0.59 Å⁻¹, 1380 independent (*R*_{int} = 0.0488) and 1178 observed reflections [*I* ≥ 2 *σ*(*I*)], 109 refined parameters, *R* = 0.0456, *wR*₂ = 0.0974 (all intensities), max. residual electron density 0.191 (−0.192) e·Å⁻³.

Compound 14b: C₁₆H₁₄N₂, *M* = 262.31, colorless plates 0.43 × 0.27 × 0.08 mm, *a* = 6.3760(6), *b* = 5.7224(5), *c* = 16.946(2) Å, *β* = 94.680(2)°, *V* = 616.21(10) Å³, *ρ*_{calc} = 1.414 g·cm⁻³, *μ* = 0.088 mm⁻¹, *Z* = 2, monoclinic space group *P*2₁/*n* (no. 14), Mo-*K*_α radiation, *λ* = 0.71073 Å, *T* = 173(2) K, 6658 reflections collected (*±h*, *±k*, *±l*), [(*sin θ*)/*λ*] = 0.70 Å⁻¹, 1767 independent (*R*_{int} = 0.0284) and 1604 observed reflections [*I* ≥ 2 *σ*(*I*)], 93 refined parameters, *R* = 0.0467, *wR*₂ = 0.12434 (all intensities), max. residual electron density 0.385 (−0.251) e·Å⁻³.

CCDC-295716 (for **9a**), -295717 (for **14a**), and -295718 (for **14b**) contain the supplementary crystallographic data for this paper. These data can be obtained free of charge from The Cambridge Crystallographic Data Centre via www.ccdc.cam.ac.uk/data_request/cif.

Computational Details: All Density Functional Theory (DFT) computations were carried out with the TURBOMOLE 5.6 program package.^[26] The ground-state geometries were optimized at the BP86/SV(P)^[27] level of theory by use of the resolution of the identity approximation^[28] for the Coulomb potential. The basis set effect on the geometry was studied for one of the transition structures **12b** by comparison with a BP86/TZVP geometry and was found to be small. The respective <*S*²> values of all investigated radicals were found to be very close to 0.75 (expected for a pure doublet state), indicating that spin contamination is of negligible importance. The transition structures were found by use of the statpt module of the TURBOMOLE package. The vibrational Hessians were obtained numerically by use of the SNF 2.2.1 program^[29] by finite differences of analytically calculated gradients. The reaction energies and activation barriers were calculated on the basis of B3-LYP/TZVP^[30] single-point energies with use of the BP86/SV(P) geometries.

- [1] N. Wiberg, *Angew. Chem.* **1968**, *80*, 809–822; *Angew. Chem. Int. Ed. Engl.* **1968**, *7*, 766–779.
- [2] M. F. Lappert, R. K. Maskell, *J. Chem. Soc., Chem. Commun.* **1982**, 580–581.
- [3] a) M. F. Lappert, *J. Organomet. Chem.* **2005**, *690*, 5467–5473.
- [4] a) M. F. Lappert, *J. Organomet. Chem.* **1988**, *358*, 185–214; b) P. B. Hitchcock, M. F. Lappert, P. L. Pye, *J. Chem. Soc., Dalton Trans.* **1978**, 826–834.
- [5] A. J. Arduengo III, J. R. Goerlich, W. J. Marshall, *J. Am. Chem. Soc.* **1995**, *117*, 11027–11028.
- [6] M. K. Denk, A. Thadani, K. Hatano, A. J. Lough, *Angew. Chem.* **1997**, *109*, 2719–2721; *Angew. Chem. Int. Ed. Engl.* **1997**, *36*, 2607–2609.

- [7] F. Demirhan, Ö. Yildirim, B. Çetinkaya, *Transition Met. Chem.* **2003**, *28*, 558–562; Y. Yamaguchi, R. Oda, K. Sado, K. Kobayashi, M. Minato, T. Ito, *Bull. Chem. Soc. Jpn.* **2003**, *76*, 991–997.
- [8] M. Alcarazo, S. J. Roseblade, E. Alonso, R. Fernández, E. Alvarez, F. J. Lahoz, J. M. Lassaletta, *J. Am. Chem. Soc.* **2004**, *126*, 13242–13243.
- [9] a) F. E. Hahn, M. Paas, D. Le Van, T. Lügger, *Angew. Chem.* **2003**, *115*, 5402–5405; *Angew. Chem. Int. Ed.* **2003**, *42*, 5243–5246; b) P. Frémont, N. M. Scott, E. D. Stevens, S. P. Nolan, *Organometallics* **2005**, *24*, 2411–2418.
- [10] W. A. Herrmann, *Angew. Chem.* **2002**, *114*, 1342–1363; *Angew. Chem. Int. Ed.* **2002**, *41*, 1290–1309.
- [11] a) T. N. Trnka, R. H. Grubbs, *Acc. Chem. Res.* **2001**, *34*, 18–29; b) S. J. Cannon, S. Blechert, *Angew. Chem.* **2003**, *115*, 1944–1968; *Angew. Chem. Int. Ed.* **2003**, *42*, 1900–1923; c) A. Fürstner, *Angew. Chem.* **2000**, *112*, 3140–3172; *Angew. Chem. Int. Ed.* **2000**, *39*, 3012–3043.
- [12] a) C.-Y. Liu, D.-Y. Chen, G.-H. Lee, S.-M. Peng, S.-T. Liu, *Organometallics* **1996**, *15*, 1055–1061; b) F. E. Hahn, V. Langenhahn, T. Pape, *Chem. Commun.* **2005**, 5390–5392; for complexes with *N,N'*-diallylbenzimidazolin-2-ylidenes see F. E. Hahn, V. Langenhahn, N. Meier, T. Lügger, W. P. Fehlhammer, *Chem. Eur. J.* **2003**, *9*, 704–712; F. E. Hahn, C. García Plumed, *Chem. Eur. J.* **2004**, *10*, 6285–6293.
- [13] J. A. Chamizo, J. Morgando, S. Bernès, *Transition Met. Chem.* **2000**, *25*, 161–165.
- [14] J. A. Chamizo, M. F. Lappert, *J. Org. Chem.* **1989**, *54*, 4684–4686.
- [15] J. A. Baldwin, S. E. Branz, J. A. Walker, *J. Org. Chem.* **1977**, *42*, 4142–4144.
- [16] B. Çetinkaya, E. Çetinkaya, J. A. Chamizo, P. B. Hitchcock, H. A. Jasim, H. Küçükbay, M. F. Lappert, *J. Chem. Soc., Perkin Trans. 1* **1998**, 2047–2054.
- [17] H. V. Huynh, N. Meier, T. Pape, F. E. Hahn, *Organometallics* **2006**, in press.
- [18] a) M. A. Walters, *J. Org. Chem.* **1996**, *61*, 978–983; b) R. F. Winter, G. Rauhut, *Chem. Eur. J.* **2002**, *8*, 641–649.
- [19] a) E. A. Goreshik, D. Schollmeyer, M. G. Mys'kiv, O. V. Pav'lyuk, *Z. Anorg. Allg. Chem.* **2000**, *626*, 1016–1019; b) E. Lukevics, P. Arsenyan, I. Shestakova, I. Domracheva, A. Nestrova, O. Pudova, *Eur. J. Med. Chem.* **2001**, *36*, 507–515.
- [20] a) F. E. Hahn, L. Wittenbecher, R. Boese, D. Bläser, *Chem. Eur. J.* **1999**, *5*, 1931–1935; b) F. E. Hahn, L. Wittenbecher, D. Le Van, R. Fröhlich, *Angew. Chem.* **2000**, *112*, 551–554; *Angew. Chem. Int. Ed.* **2000**, *39*, 541–544.
- [21] a) F. E. Hahn, T. von Fehren, L. Wittenbecher, R. Fröhlich, *Z. Naturforsch., Teil B* **2004**, *59*, 541–543; b) F. E. Hahn, T. von Fehren, L. Wittenbecher, R. Fröhlich, *Z. Naturforsch., Teil B* **2004**, *59*, 544–546; c) F. E. Hahn, T. von Fehren, *Inorg. Chim. Acta* **2005**, *358*, 4137–4144.
- [22] a) F. E. Hahn, M. Foth, *J. Organomet. Chem.* **1999**, *585*, 241–245; b) F. E. Hahn, C. Holtgrewe, T. Pape, *Z. Naturforsch., Teil B* **2004**, *59*, 1051–1053; c) F. E. Hahn, C. Holtgrewe, T. Pape, M. Martin, E. Sola, L. A. Oro, *Organometallics* **2005**, *24*, 2203–2209.
- [23] a) K. L. Tan, R. G. Bergman, J. A. Ellman, *J. Am. Chem. Soc.* **2001**, *123*, 2685–2686; b) A. H. Velders, A. C. G. Hotze, J. Redijk, *Chem. Eur. J.* **2005**, *11*, 1325–1340.
- [24] N. Rath, R. R. Mohanty, H. Hemling, *Indian J. Heterocycl. Chem.* **1997**, *6*, 303–312.
- [25] G. M. Sheldrick, SHELXL-97, University of Göttingen, Germany, **1997**.
- [26] R. Ahlrichs, M. Bär, H.-P. Baron, R. Bauernschmitt, S. Böcker, M. Ehrig, K. Eichkorn, S. Elliott, F. Furche, F. Haase, M. Häser, H. Horn, C. Huber, U. Huniar, M. Kattannek, C. Kölmel, M. Kollwitz, K. May, C. Ochsenfeld, H. Öhm, A. Schäfer, U. Schneider, O. Treutler, M. von Arnim, F. Weigend, P. Weiss, H. Weiss, TURBOMOLE, University of Karlsruhe, **2003**.

- [27] a) J. P. Perdew, *Phys. Rev. B* **1986**, 33, 8822–8824; b) A. D. Becke, *Phys. Rev. A* **1988**, 38, 3098–3100; c) A. Schäfer, H. Horn, R. Ahlrichs, *J. Chem. Phys.* **1992**, 97, 2571–2577.
- [28] K. Eichkorn, O. Treutler, H. Ohm, M. Häser, R. Ahlrichs, *Chem. Phys. Lett.* **1995**, 240, 283–289.
- [29] C. Kind, M. Reiher, J. Neugebauer, B. Hess, SNF, version 2.2.1, University of Erlangen, **1999–2002**.
- [30] a) A. D. Becke, *J. Chem. Phys.* **1993**, 98, 5648–5652; b) C. Lee, W. Yang, R. G. Parr, *Phys. Rev. B* **1988**, 37, 785–789; c) A. Schäfer, C. Huber, R. Ahlrichs, *J. Chem. Phys.* **1994**, 100, 5829–5835; d) P. J. Stephens, F. J. Devlin, C. F. Chabalowski, *J. Phys. Chem.* **1994**, 98, 11623–11627.

Received: February 1, 2006
Published Online: May 10, 2006